2013 IEEE/ASME International Conference on
Advanced Intelligent Mechatronics (AIM)
Wollongong, Australia, July 9-12, 2013

Design and Postural Synergy Synthesis of a Prosthetic Hand for a Manipulation Task

Kai Xu*, *Member, IEEE*, Jiangran Zhao, *Student Member, IEEE*,
Yuheng Du, Xinjun Sheng, *Member, IEEE*, and Xiangyang Zhu, *Member, IEEE*

***Abstract*— Recent advances in neurology showed that human controls muscles for hand poses in a coordinated manner. This coordination is referred as to a postural synergy. Using postural synergies, a few synergy inputs (usually two) can be used to control dozens of motors to accomplish various grasping tasks on a prosthetic robotic hand. This paper presents the latest results of a project which attempts to achieve delicate motions (e.g. manipulation of objects) on a prosthetic hand using two synergy inputs. In order to better reproduce the desired poses for the manipulation task, the postural synergies were synthesized on a kinematically identical dummy hand. The prosthetic hand was designed, fabricated and assembled. Tests were performed to qualitatively verify motion ranges of the prosthetic hand. Experimentation that follows is expected to demonstrate the completion of the intended manipulation tasks.**

I. Introduction

It is a particularly challenging task to build and attach an anthropomorphic prosthetic hand that can replicate delicate motions of the biological original. In order to achieve this goal, the prosthetic hand shall be versatile enough for various daily tasks and controllable through a bio-signal interface, such as EMG (electro-myography) or EEG (electro-encephalography). However limited bandwidth of these interfaces used to prevent fully actuated robotic hands from being applied as prostheses if each DoF (Degree of Freedom) requires individual control to perform dexterous grasping tasks, even though many designs were absolutely the state-of-the-art (e.g. the ones in [1-4]).

Recent advances in neurology may have solved this puzzle. It was showed that CNS (Central Nervous System) controls hand muscles in a coordinated manner. This coordination is referred as to a postural synergy. Each postural synergy corresponds to flexion/extension actuation statuses of several involved muscles. CNS combines postural synergies, adjusting each synergy's weight (coefficient), to realize various hand motions. Combination of two primary postural synergies accounts for about 84% of the variance of dozens of different grasping postures [5]. What's more, CNS switches between different sets of postural synergies for distinct grasping and manipulations tasks [6].

This work was supported by the Chinese National Program on Key Basic Research Projects (the 973 Program) #2011CB013300.

Kai Xu, Jiangran Zhao and Yuheng Du are with the RII Lab (Lab of Robotics Innovation and Intervention), UM-SJTU Joint Institute, Shanghai Jiao Tong University, Shanghai, China (asterisk indicates the corresponding author, phone: 8621-34207220; fax: 8621-34206525; emails: k.xu@sjtu.edu.cn, zjr318@sjtu.edu.cn, and jhdyh1991@sjtu.edu.cn).

Xinjun Sheng and Xiangyang Zhu are with the School of Mechanical Engineering, Shanghai Jiao Tong University, Shanghai, China (emails: xjsheng@sjtu.edu.cn and mexyzhu@sjtu.edu.cn).

These findings enabled control of robotic hands with many actuators via a few inputs. These inputs are coefficients while combining postural synergies. For example, two and three postural synergies were used to control 24 actuators in the ACT hand to perform writing and piano playing [7, 8]. Other examples include the use of two synergies in the DLR II hand [9], the use of three synergies in the SAH hand [10], the use of two synergies in the UB hand [11], etc.

Unlike referring to the discrete grasp taxonomy as in [12-14], the concept of postural synergies introduced a new approach for grasp planning. As shown in a milestone work done by Ciocarlie and Allen [15], poses of different hands could be optimized to achieve various grasping tasks. Since two synergy inputs can be adjusted to grasp distinct objects, they might also be used to manipulate the same object (manipulation of one object is essentially a smooth transition between different grasping patterns of the same object). There is a great possibility of realizing more delicate motions on a postural-synergy-controlled prosthetic hand, upgrading its motion capability from object grasping to object manipulation.

This paper attempts to demonstrate the possibility of such an upgrade, by presenting the design of a prosthetic hand and postural synergy synthesis using a dummy hand. The entire project aims at realizing the object manipulation under the control of two synergy inputs, as shown in Fig. 1, whereas this paper focuses on mechanical design and synergy synthesis of this hand. The specific motion paradigm is the manipulation of two rehabilitation training balls on the palm in a cyclic pattern.

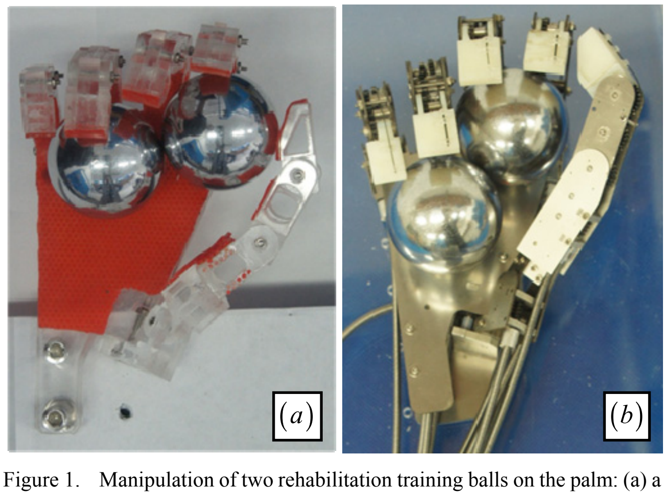

Figure 1. Manipulation of two rehabilitation training balls on the palm: (a) a pose of the dummy hand and (b) a pose of the prosthetic hand

Postural synergies are usually extracted as the first a few (usually two) principal components from recorded joint angles of a hand under many poses. Then the synergies are translated into a prosthetic hand's controller to map the synergy inputs to the actuator outputs. When grasping tasks were performed as in [9-11, 15], the synergy inputs were adjusted to properly form poses of the hand. These adjustments essentially compensated for the discrepancy between the original postural synergies and their implementations in the controllers. When manipulation tasks are intended for a prosthetic hand, the synergy inputs will be primarily used to transform the hand from one pose to another in a continuous manner, limiting their play in compensating/correcting the implemented postural synergies. Hence, synergy discrepancy should be minimized for the prosthetic hand to satisfactorily reproduce the specific sequenced motions via only two synergy inputs.

In order to address the challenge of minimizing synergy discrepancy, this paper introduces a novel technique of constructing a dummy hand for the synthesis of postural synergies. Instead of inviting 5 to 10 human subjects, asking them to manipulate rehabilitation training balls, recording and analyzing the human hand motions using sophisticated systems such as CyberGlove™ or Vicon™ cameras, this dummy hand was built and manually posed to manipulate the training balls with each pose measured. Constructing a dummy hand and measuring its poses will be shown to produce direct results for synergy synthesis of the prosthetic hand in a very cost-efficient way. More importantly it avoided unnecessary discrepancies while designing prosthetic mechanisms with lower kinematic pairs (e.g. prismatic & revolute joints) based on measurements of human hands whose joints are essentially higher kinematic pairs (e.g. carpometacarpal joint, metacarpophalangeal joints).

The main contribution of this paper is the proposal of perform postural synergy synthesis using a dummy hand for more direct and accurate results. The minor contributions of this work include the structural designs and the transmission schemes of the presented prosthetic hand.

The paper is organized as follows. Section II presents the synthesis of the postural synergies using a dummy hand. Section III presents the mechanism designs of a prosthetic hand whose kinematic parameters and enveloping dimensions are identical to those of the dummy hand. Section IV presents preliminary experimental results with the conclusion and the future work followed in Section V.

II. Postural Synergy Synthesis

This paper proposes to enable multi-finger manipulation on a prosthetic hand under the control of two synergy inputs. The intended paradigm is to rotate two rehabilitation training balls on palm using coordinated finger motions as shown in Fig. 1. This exercise helps the elderly or patients after mild stroke to maintain or recover their hand motor function. Although this motion sequence might not seem practically meaningful to amputees, the motivation here is to demonstrate the capability and effectiveness of this presented design process.

In order to realize this specific motion sequence on an under-controlled prosthetic hand, a dummy hand was firstly constructed as shown in Fig. 2-(a). All the joints were passive with friction big enough to hold them still against external disturbance (e.g. gravity). The arrangement of its revolute joints provided motion capabilities similar to a human hand but also left enough space to realize actuations of these joints. The dummy hand had identical enveloping dimensions and geometry as the one to be constructed with transmissions and actuations in Fig. 1-(b). The rest of this section obtained, adjusted and finalized the postural synergies from a continuous hand motion of manipulating two rehabilitation training balls. Then design of structures, transmissions and actuations of the prosthetic hand was carried out in Section III.

A. Original Postures and Raw Synergies

In order to realize the intended motion of manipulating rehabilitation training balls on a prosthetic hand, a dummy hand shown in Fig. 2-(a) was constructed and manually posed for six different key poses as shown in Fig. 3-(a)~(f). Joints of this dummy hand are indicated in Fig. 2-(a) with their angle values and motion ranges summarized in Table 1. The joints are named as follows. Letters *T*, *M*, *R*, *L* and *I* before the underscore indicate the joints for the thumb, the middle finger, the ring finger and the little finger respectively. Abbreviations of *rot*, *mcp*, *ip*, *abd*, *pip* and *dip* after the underscore indicate the rotation joint, the metacarpophalangeal joint, the interphalangeal joint, the abduction joint, the proximal and the distal interphalangeal joint respectively.

TABLE I. JOINT RANGES AND JOINT ANGLES OF THE DUMMY HAND IN THE KEY POSES IN FIG. 2

Joints	Joint limits (°)	Joint angles (°) in poses in Fig. 3					
		(a)	(b)	(c)	(d)	(e)	(f)
T_rot	[0, 135]	48	44	37	65	87	69
T_mcp	[0, 90]	24	36	42	45	50	35
T_ip	[0, 90]	29	40	50	50	55	40
T_abd	[0, 80]	30	38	43	52	55	40
I_mcp	[0, 90]	45	58	75	50	25	16
M_mcp	[0, 90]	55	43	45	1	4	21
R_mcp	[0, 90]	55	50	41	0	17	52
L_mcp	[0, 90]	55	50	73	50	55	55
I_pip	[0, 100]	59	54	52	55	53	56
M_pip	[0, 100]	63	85	69	77	69	69
R_pip	[0, 100]	75	69	70	72	73	76
L_pip	[0, 100]	71	65	57	80	69	78
I_abd	[0, 20]	5	10	10	5	5	17
R_abd	[0, 20]	5	10	8	13	10	12
L_abd	[0, 20]	15	19	10	16	15	18
I_dip	[0, 45]	58	53	52	55	53	56
M_dip	[0, 45]	45	61	50	55	50	50
R_dip	[0, 45]	38	35	35	36	37	38
L_dip	[0, 45]	36	33	29	40	35	39

For all the interphalangeal joints and metacarpophalangeal joints, zero values are defined as they reach their full extensions whereas positive values are defined for flexion motions. For all the abduction joints, positive values are defined in their abduction motions. Abduction joint of the middle finger is fixed, since abduction motions are measured relatively. Positive value of the thumb rotation joint is defined in its opposition motion. In total there are 19 joints in the dummy hand (excluding the abduction joint of the middle finger). This corresponds to the 19 rows in Table 1.

In each pose, joint angles were measured using an optical tracker (MicronTracker SX60 from Claron Technology Inc) as shown in Fig. 3-(h). Two adjacent intersecting surfaces of the two adjacent phalanxes was first characterized by obtaining coordinates of three or more points on the surfaces (The surfaces were characterized in the tracker frame), as shown in Fig. 2-(b). The joint angle was then obtained from the dot product of the two surface normals. Joint values of these six key poses are listed in Table 1.

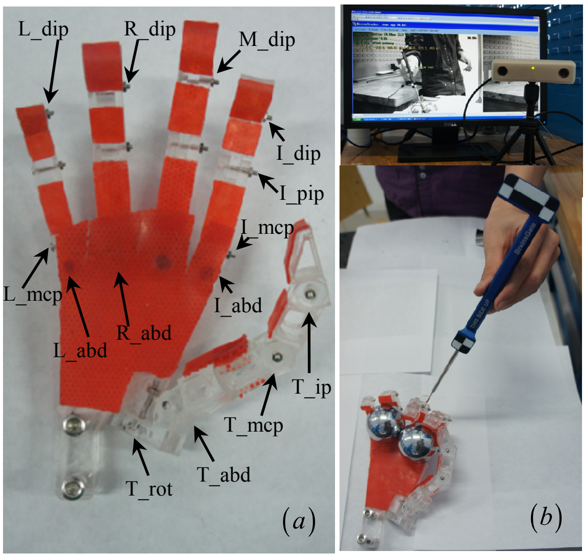

Figure 2. (a) Construction of the dummy hand; (b) Measurement process of the joint angles using an optical tracker

Each pose in Fig. 3-(a)~(f) corresponds to a pose vector $\mathbf{p}_i \in \Re_{19\times 1}$, $i = 1, 2, \cdots, 6$. According to Table 1, it should be noticed that motions of the four distal interphalangeal joints (I_dip, M_dip, R_dip and L_dip) were coupled to the motions of the four proximal interphalangeal joints (I_pip, M_pip, R_pip and L_pip). Hence dimension of the pose vector can be further reduced to 15, namely $\mathbf{p}_i \in \Re_{15\times 1}$, whereas the coupling between the distal interphalangeal joints and the proximal interphalangeal joints is as follows:

$$\begin{array}{ll} p_{I\_dip} = p_{I\_pip} & p_{M\_dip} = 0.72 p_{M\_pip} \\ p_{R\_dip} = 0.5 p_{R\_pip} & p_{L\_dip} = 0.5 p_{L\_pip} \end{array} \tag{1}$$

It will be shown in the next section that these coupling coefficients will all be accommodated by the transmission designs in the prosthetic hand.

Six poses in Fig. 3-(a)~(f) can be put side to side to form a pose matrix $\mathbf{P}$ (numerical values of $\mathbf{P}$ are listed in Table 1):

$$\mathbf{P}_{15\times 6} = \begin{bmatrix} \mathbf{p}_1 & \mathbf{p}_2 & \cdots & \mathbf{p}_6 \end{bmatrix} \tag{2}$$

The concept of implementing postural synergies is to use less control inputs to realize this hand pose sequence, even though each pose involves rotations of 15 hand joints (19 joints counting the coupled ones). If only two control inputs are expected, an ideal scenario is that the pose matrix $\mathbf{P}$ is rank 2 and all $\mathbf{p}_i$ can be linearly spanned using two basis vectors. In order to examine how close the actual matrix $\mathbf{P}$ is to the ideal case, singular value decomposition was introduced:

$$\begin{aligned} \mathbf{P} &= \bar{\mathbf{P}} + \mathbf{U}_{15\times 15} \mathbf{\Sigma}_{15\times 6} \mathbf{V}_{6\times 6}^T \\ &= \bar{\mathbf{P}} + \begin{bmatrix} \mathbf{u}_1 & \mathbf{u}_2 & \cdots & \mathbf{u}_{15} \end{bmatrix} \cdot \begin{bmatrix} \operatorname{diag}(\delta_1, \delta_2, \cdots, \delta_6) \\ \mathbf{0}_{9\times 6} \end{bmatrix} \begin{bmatrix} \mathbf{v}_1^T \\ \mathbf{v}_2^T \\ \vdots \\ \mathbf{v}_6^T \end{bmatrix} \end{aligned} \tag{3}$$

Where $\bar{\mathbf{P}} = \begin{bmatrix} \bar{\mathbf{p}} & \bar{\mathbf{p}} & \bar{\mathbf{p}} & \bar{\mathbf{p}} & \bar{\mathbf{p}} & \bar{\mathbf{p}} \end{bmatrix}$ is the average pose matrix, $\bar{\mathbf{p}} = \frac{1}{6}\sum_{i=1}^{6} \mathbf{p}_i$ and $\mathbf{v}_i^T \in \Re_{1\times 6}$.

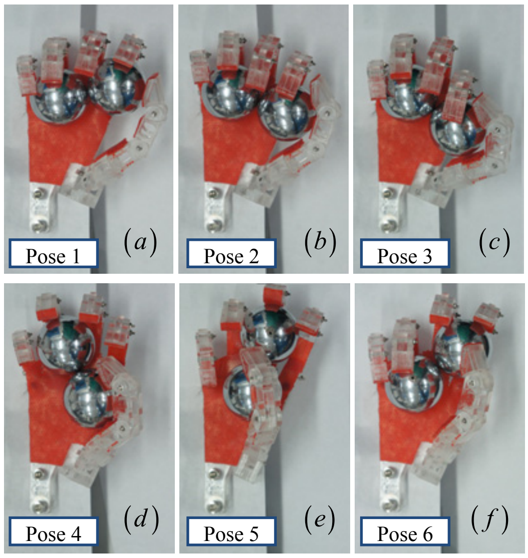

Figure 3. Six key poses for the dummy hand to manipulate two rehabilitation training balls in a cyclic pattern

If the singular values δ_i ($i = 3, 4, 5, 6$) are small enough to be neglected, the pose matrix $\mathbf{P}$ can be approximated by an approximate pose matrix $\tilde{\mathbf{P}}$:

$$\tilde{\mathbf{P}} = \bar{\mathbf{P}} + \begin{bmatrix} \mathbf{u}_1 & \mathbf{u}_2 \end{bmatrix} \begin{bmatrix} \delta_1 \mathbf{v}_1^T \\ \delta_2 \mathbf{v}_2^T \end{bmatrix} \tag{4}$$

Eq. (4) can be rewritten as Eq. (5) so that each hand pose can be approximated as in Eq. (6):

$$\tilde{\mathbf{P}} = \bar{\mathbf{P}} + \begin{bmatrix} \mathbf{u}_1 & \mathbf{u}_2 \end{bmatrix} \begin{bmatrix} q_{11} & q_{12} & \cdots & q_{16} \\ q_{21} & q_{22} & \cdots & q_{26} \end{bmatrix} \tag{5}$$

$$\tilde{\mathbf{p}}_i = \bar{\mathbf{p}} + q_{1i} \mathbf{u}_1 + q_{2i} \mathbf{u}_2, \; i = 1, 2, \cdots, 6 \tag{6}$$

Vectors $\mathbf{u}_1$ and $\mathbf{u}_2$ are referred to as postural synergies. With q_{1i} and q_{2i} as synergy inputs, various hand poses could be approximated when the two postural synergies are combined in the prosthetic hand's controller.

Since the poses were only approximated, a pose error matrix $\mathbf{P}_{error}$ can be defined as the following:

$$\mathbf{P}_{error} = \mathbf{P} - \tilde{\mathbf{P}} \tag{7}$$

This pose error matrix $\mathbf{P}_{error}$ can be visualized in Fig. 4, where X and Y axes stand for joints and poses (e.g. there are 15 joints in one pose) with Z axis standing for the errors in the joints under different poses. The biggest error is about 12.8° and norm of these errors is 26.26°.

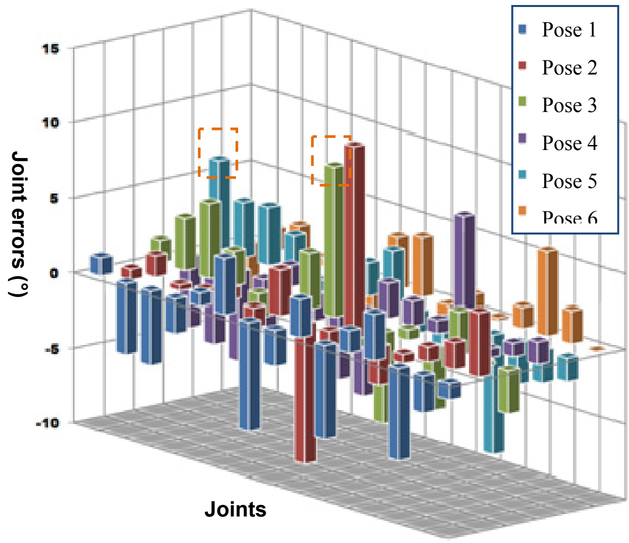

Figure 4. Visualization of the pose error matrix with critical errors marked

B. Adjusted Poses and Postural Synergies

Although manipulating the two rehabilitation training balls is a complicated task, the errors from Eq. (7) are not equally important. Some errors corresponded to fingers that even didn't touch either of the balls. However, two critical errors were identified in Fig. 4:

- One error belongs to the L_mcp joint of Pose 3 as in Fig.3-(c). Numerical value of this error is +10°. According to the definition of the errors from Eq. (7), an error of +10° means this joint rotated 10° less. Referring to Fig.3-(c), this error is critical because the little finger will not be able to push the left-upper ball towards the right side, if the L_mcp joint rotates less than the desired value.
- The other critical error belongs to the T_rot joint of Pose 5 as in Fig.3-(e). Numerical value of this error is +6°, meaning this joint rotated 6° less. Referring to Fig.3-(d)~(e), this error is critical because the thumb will not be able to push the right-lower ball towards the left side, if the T_rot joint doesn't rotate enough.

In order to reduce the critical errors, two joint values were adjusted: for the L_mcp joint of Pose 3 as in Fig.3-(c), joint angle was increased from 73° to 85°; for the T_rot joint of Pose 5 as in Fig.3-(e), joint angle was increased from 87° to 95°. Then the procedure from Eq. (3) to Eq. (7) was repeated, the following new entities were obtained, including a new pose matrix $\mathbf{P}'$, a new average pose matrix $\bar{\mathbf{P}}'$, a new approximate pose matrix $\tilde{\mathbf{P}}'$, new postural synergies $\mathbf{u}'_i$ ($i = 1,2$), new inputs q'_{ki} ($i = 1,2$, $k = 1,2,\cdots,6$), and a new pose error matrix $\mathbf{P}'_{error}$. $\mathbf{P}'_{error}$ was visualized again as in Fig.5. From this figure, critical errors were diminished, even though the error with the biggest absolute value rose to 13.2° with norm of these errors of 27.01°. The new average pose vector $\bar{\mathbf{p}}'$, new postural synergies $\mathbf{u}'_i$ ($i = 1,2$), and new inputs q'_{ki} ($i = 1,2$, $k = 1,2,\cdots,6$) are also summarized in Table 2 with the relation among them as the following:

$$\tilde{\mathbf{P}}' = \bar{\mathbf{P}}' + [\mathbf{u}'_1 \quad \mathbf{u}'_2] \begin{bmatrix} q'_{11} & q'_{12} & \cdots & q'_{16} \\ q'_{21} & q'_{22} & \cdots & q'_{26} \end{bmatrix} \tag{8}$$

Pose adjustments presented here could be analytically formulated as an optimization problem, aiming at reducing specific or critical errors. It is not necessary to strictly stick to the measured original poses as far as the regenerated approximate poses better fulfill the goals.

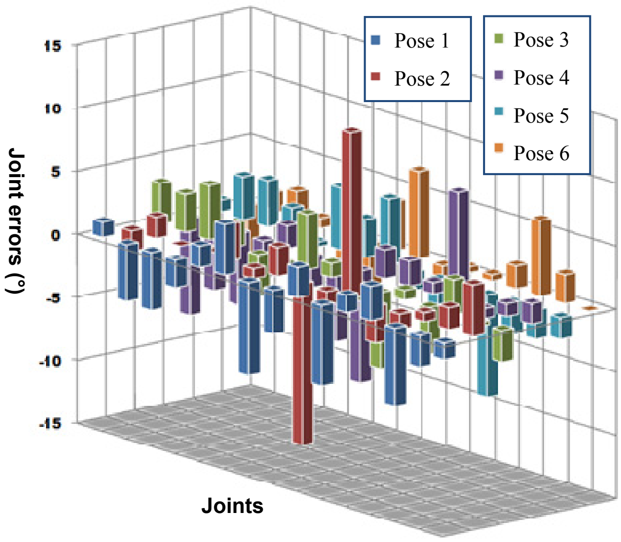

Figure 5. Visualization of the adjusted pose error matrix

III. Hand Design Descriptions

According to Eq. (8), two synergy inputs q'_{k1} and q'_{k2} ($k = 1,2,\cdots,6$) shall be combined, scaled and mapped to 15 actuator outputs in the controller to drive the prosthetic hand from its average pose $\bar{\mathbf{p}}'$. Since it is unlikely all the desired actuators could be fully embedded in the palm, actuators (motors) are planned for installation in the forearm, as shown in Fig. 6. A straightforward way to connect these motor outputs to the finger joints is to use flexible shafts. Using flexible shafts brings an addition benefit that their rotations would not be affected by a possible presence of wrist motions. Using worm gears and gears, rotations of these flexible shafts will drive all the finger joints.

Since the dummy hand was posed for the desired motion sequence of manipulating two rehabilitation training balls, kinematics arrangement (e.g. arrangement of the joint axes) and enveloping dimensions of this prosthetic hand must remain as identical as possible to the dummy hand. This section focused on how to incorporate transmissions and actuations within the available space to drive all the 19 joints of this hand (the abduction joint of the middle finger was fixed). Main design components include i) transmission and actuation of the thumb, ii) those of the fingers, and iii) actuation of the abduction motions between the fingers.

TABLE II. THE AVERAGE POSE, THE POSTURAL SYNERGIES AND THE SYNERGY INPUTS OF THE ADJUSTED POSES

Joints	Average pose (°)	Postural synergies	
		$\mathbf{u}'_1$	$\mathbf{u}'_2$
T_rot	59.7	-0.49	0.24
T_mcp	38.7	-0.16	-0.21
T_ip	44.0	-0.15	-0.23
T_abd	43.0	-0.2	-0.17
I_mcp	44.8	0.34	-0.66
M_mcp	28.2	0.56	0.12
R_mcp	35.8	0.44	0.5
L_mcp	58.3	0.15	-0.25
I_pip	54.8	0.01	0.06
M_pip	72.0	-0.01	-0.11
R_pip	72.5	-0.02	0.08
L_pip	70	-0.13	0.14
I_abd	8. 7	0.03	0.08
R_abd	9. 7	-0.05	-0.02
L_abd	15.5	-0.02	0.07

Pose 1 inputs (°)		Pose 2 inputs (°)		Pose 3 inputs (°)	
q'_{11}	36.2	q'_{12}	28.1	q'_{13}	37.6
q'_{21}	21.0	q'_{22}	-1.1	q'_{23}	-31.5
Pose 4 inputs (°)		**Pose 5 inputs (°)**		**Pose 6 inputs (°)**	
q'_{14}	-38.5	q'_{15}	-52.4	q'_{16}	-11.0
q'_{24}	-25.1	q'_{25}	2.6	q'_{26}	34.1

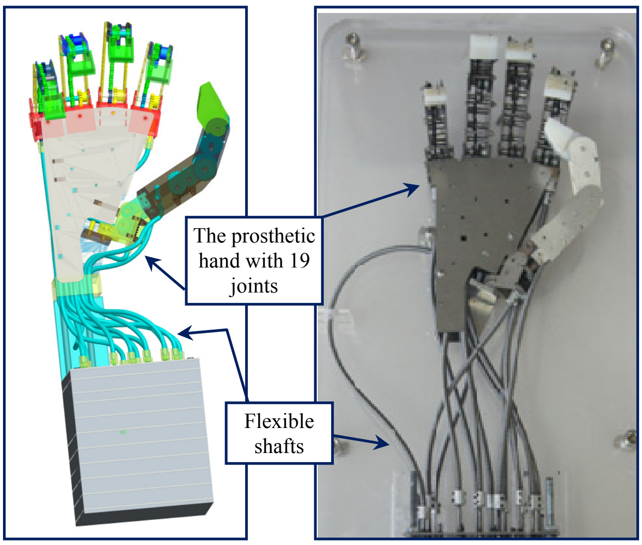

Figure 6. Design overview: the motor outputs connected to the prosthetic hand via flexible shafts

A. Transmission and Actuation of the Thumb

As mentioned above, flexible shafts were used to transmit rotary outputs to drive the hand joints. As shown in Fig. 7, flexible shafts were connected to the worms to the drive worm gears. Then the worm gears were attached to a train of spur gears to actuate the T_rot, T_abd, T_mcp and T_ip joints. The train of spur gears was used to allow proper positioning of the worms and worm gears so that they could be fully housed inside the thumb. All the worms used in the prosthetic hand had only 1 start and all the worm gears had 20 teeth.

As shown in Fig. 7, a dual arrangement of worm gears introduced coupling between the T_mcp and the T_ip joints. Once the worm gear for the T_mcp joint was actuated, in order to keep the thumb distal phalanx stationary with respect to the thumb proximal phalanx, the worm gear for the T_ip joint should be actuated accordingly. This coupling should be accommodated in the controller.

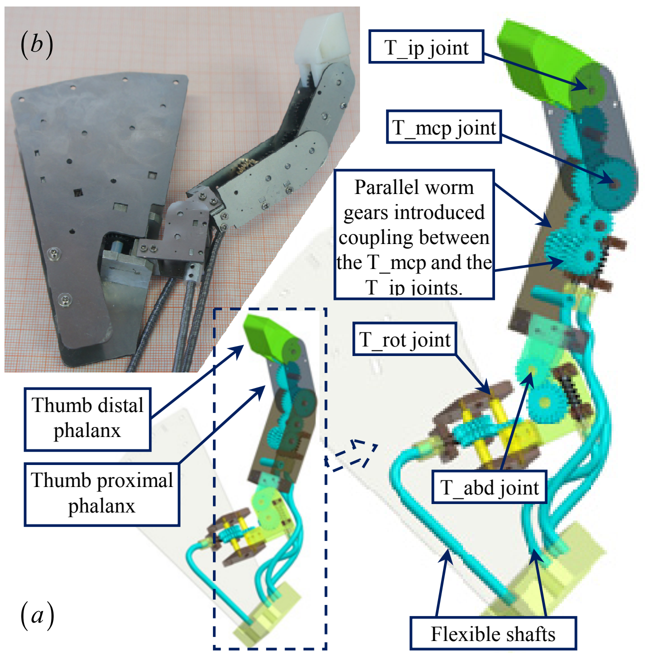

Figure 7. Transmission and actuations of the thumb: (a) the CAD model; (b) the actual subassembly

B. Actuation of the Fingers

Similar to the actuation of the thumb T_mcp and T_ip joints, flexible shafts were connected to the worms & worm gears and the trains of spur gears to drive the metacarpophalangeal and interphalangeal joints. Since actuation of the index, the middle, the ring and the little fingers are essentially similar, Fig. 8 only shows the structure of the middle finger. Coupling between the distal interphalangeal joint and the proximal interphalangeal joint was realized using trains of spur gears inside the fingers. As shown in Fig. 8, two gears (the green one and the dark blue one) were attached so that the green gear train actuated the distal phalanx and the dark blue gear train actuated the proximal phalanx. Gear ratios were selected to realize the coupling between the M_dip joint and the M_pip joint according to Eq. (1). Please note that these gear trains can be adjusted to realize different coupling for the index, the ring and the little fingers. Axes of these gears were offset to accommodate their specific pitch radiuses.

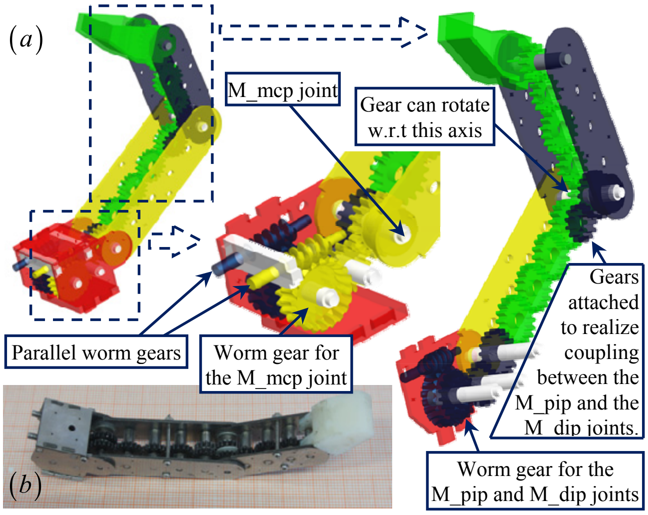

Figure 8. Actuation of the middle joint: (a) the CAD model; (b) the actual subassembly

C. Actuation of the Finger Abduction Joints

According to Eq. (8) and Table 2, abduction motions of the index, the ring and the little fingers were also subjected to inputs q'_{k1} and q'_{k2} , which means three more motors would be needed. However, their synergies values (abd rows for $\mathbf{u}'_i$) are substantially smaller than those of other joints, because they rotated much less than other joints. In order to reduce the number of motors, abduction motions of the three fingers were made coupled. Gear profiles were fabricated on components of the finger subassemblies so that one set of worm & worm gear will drive abduction motions of the index, the ring and the little fingers through a train of spur gears.

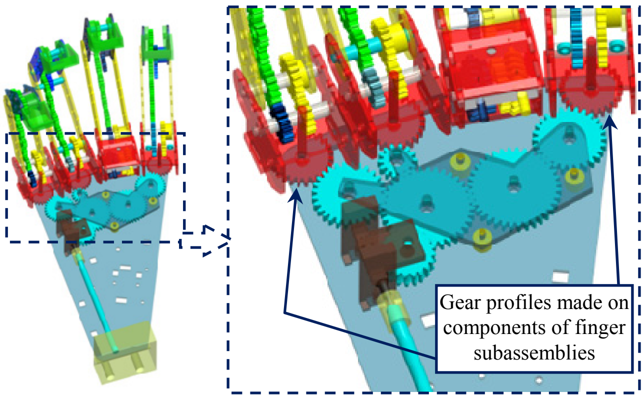

Figure 9. Abduction motions were made coupled for the index, the ring and the little fingers

IV. Preliminary Experimental Results

All the components of the prosthetic hand were fabricated and assembled. Four rotations are needed for the T_rot, the T_abd, the T_mcp and the T_ip joints of the thumb. Two rotations are needed for the metacarpophalangeal joint and the proximal interphalangeal joint of the four fingers (their distal interphalangeal joints are actuated by the proximal interphalangeal joints though couple gear trains). One more rotation is needed for the abductions of the fingers. In total, 13 rotations are needed to drive the 19 joints in the prosthetic hand (abduction of the middle finger is fixed).

Before an actuation and control system with 19 rotary outputs are constructed, the prosthetic hand was manually posed by rotating its flexible shafts, to verify motion ranges of the joints. As shown in Fig. 10, the prosthetic hand can be successfully posed for the six key postures which are needed for manipulating the two rehabilitation training balls in a cyclic manner. Comparing to the poses in Fig. 3, obviously there are discrepancy and errors between the poses of the dummy hand and that of the prosthetic hands. In fact the six poses in Fig. 3 don't guarantee that the continuous manipulation of two training balls will be realized. The experiments performed here mainly tried to show motion ranges of the prosthetic hands to qualitatively verify its capability for this intended task. Further experimentation will be carried out on critical aspects of realizing this intended task, such as inter-pose trajectory planning, backlash compensation, etc.

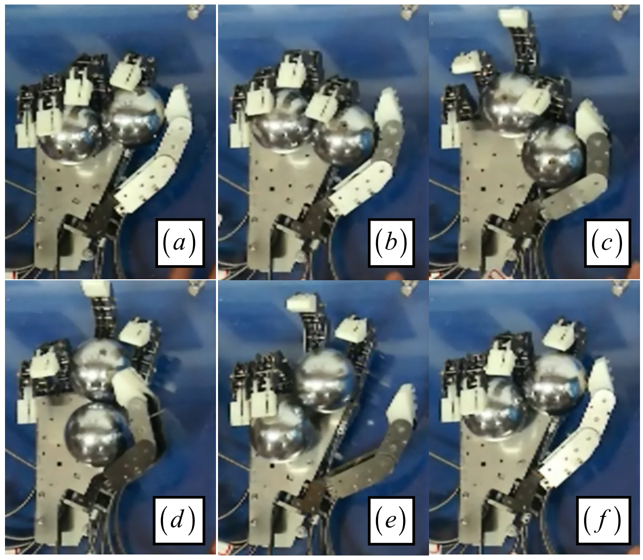

Figure 10. The assembled prosthetic hand was manually posed by rotating the flexible shafts to qualitatively verify its motion capability for the intended task of manipulating two training balls in a cyclic manner.

V. Conclusion and Future Work

This paper presented the latest results of a prosthetic hand project regarding its mechanical structural design and the postural synergy synthesis. This project attempts to upgrade motion capability of a prosthetic hand from object grasping to more delicate motions (such as manipulation of objects). A specific manipulation paradigm was selected as the manipulation of two rehabilitation training balls in a cyclic manner using two synergy inputs.

A dummy hand was constructed and manually posed for posture measurements for the synthesis of postural synergies. Then the synergy-based control will be carried out on a prosthetic hand with actual transmissions and actuations whose kinematic parameters and enveloping dimensions are identical to those of the dummy hand. This novel technique avoided the discrepancy while designing the prosthetic hand with lower kinematic pairs (e.g. prismatic & revolute joints) based on measurements of human hands whose joints are essentially higher kinematic pairs (e.g. carpometacarpal joint, metacarpophalangeal joints).

Using this technique, the poses of the dummy hand could be accurately repeated by the prosthetic hand using the corresponding postural synergies and synergy inputs. Then these synergy inputs will have more play to transform the poses of the prosthetic hand from one to another continuously.

The prosthetic hand was designed, fabricated and assembled. Preliminary experiments were performed to qualitatively verify joint motions of the prosthetic hand.

Future work includes several aspects. The first aspect is to construct a servo-control system with 13 motors so that synergy-based control can be actually carried out on the prosthetic hand. Secondly planning of the synergy inputs will be investigated, trying to realize the proposed manipulation task in a continuous manner. Thirdly, motion capabilities of additional grasping and manipulating tasks will be explored using the same sets of postural synergies.

ACKNOWLEDGMENT

The authors would like to thank Tao Xu, Tianwei Wang and Xueying Hou from the UM-SJTU Joint Institute, Shanghai Jiao Tong University, for their help in generating technical drawings and assembling the hand.

REFERENCES

[1] A. Bicchi, "Hands for Dexterous Manipulation and Robust Grasping: a Difficult Road toward Simplicity," *IEEE Transactions on Robotics and Automation,* vol. 16, No.6, pp. 652-662, Dec 2000.

[2] J. P. Gazeau, S. Zeghloul, M. Arsicault, and J. P. Lallemand, "The LMS Hand : Force and Position Controls in the Aim of the Fine Manipulation of Objects," in *IEEE International Conference on Robotics and Automation (ICRA)*, Seoul, Korea, 2001.

[3] H. Liu, P. Meusel, N. Seitz, B. Willberg, G. Hirzinger, M. H. Jin, Y. W. Liu, R. Wei, and Z. W. Xie, "The Modular Multisensory DLR-HIT-Hand," *Mechanism and Machine Theory,* vol. 42, No.5, pp. 612-625, May 2007.

[4] M. Grebenstein, M. Chalon, W. Friedl, S. Haddadin, T. Wimböck, G. Hirzinger, and R. Siegwart, "The Hand of the DLR Hand Arm System: Designed for Interaction," *International Journal of Robotics Research,* vol. 31, No.13, pp. 1531-1555, 2012.

[5] M. Santello, M. Flanders, and J. F. Soechting, "Postural Hand Synergies for Tool Use," *The Journal of Neuroscience,* vol. 18, No.23, pp. 10105-10115, Dec 1998.

[6] E. J. Weiss and M. Flanders, "Muscular and Postural Synergies of the Human Hand," *Journal of Neurophysiology,* vol. 92, No.1, pp. 523-535, 2004.

[7] E. Rombokas, M. Malhotra, and Y. Matsuoka, "Task-specific Demonstration and Practiced Synergies for Writing with the ACT Hand," in *IEEE International Conference on Robotics and Automation (ICRA)*, Shanghai, China, 2011, pp. 5363-5368.

[8] A. Zhang, M. Malhotra, and Y. Matsuoka, "Musical Piano Performance by the ACT Hand," in *IEEE International Conference on Robotics and Automation (ICRA)*, Shanghai, China, 2011, pp. 3536-3541.

[9] T. Wimböck, B. Jahn, and G. Hirzinger, "Synergy Level Impedance Control for Multifingered Hands," in *IEEE/RSJ International Conference on Intelligent Robots and Systems (IROS)*, San Francisco, CA, USA, 2011, pp. 973-979.

[10] J. Rosell, R. Suárez, C. Rosales, and A. Pérez, "Autonomous Motion Planning of a Hand-Arm Robotic System Based on Captured Human-like Hand Postures," *Autonomous Robots,* vol. 31, No.1, pp. 87-102, 2011.

[11] F. Ficuciello, G. Palli, C. Melchiorri, and B. Siciliano, "Experimental evaluation of Postural Synergies during Reach to Grasp with the UB Hand IV," in *IEEE/RSJ International Conference on Intelligent Robots and Systems (IROS)*, San Francisco, CA, USA, 2011, pp. 1775-1780.

[12] M. R. Cutkosky, "On Grasp Choice, Grasp Models, and the Design of Hands for Manufacturing Tasks," *IEEE Transactions on Robotics and Automation,* vol. 5, No.3, pp. 269-279, June 1989.

[13] T. Feix, R. Pawlik, H.-B. Schmiedmayer, J. Romero, and D. Kragić, "A Comprehensive Grasp Taxonomy," in *Robotics, Science and Systems Conference (RSS)*, Seattle, Washington, USA, 2009.

[14] J. Z. Zheng, S. De La Rosa, and A. M. Dollar, "An Investigation of Grasp Type and Frequency in Daily Household and Machine Shop Tasks," in *IEEE International Conference on Robotics and Automation (ICRA)*, Shanghai, China, 2011, pp. 4169-4175.

[15] M. T. Ciocarlie and P. K. Allen, "Hand Posture Subspaces for Dexterous Robotic Grasping," *The International Journal of Robotics Research,* vol. 28, No.7, pp. 851-867, June 2009.